

Chaotic Dynamics in a Periodically Excited Air Jet

Marco Bonetti

Von Karman Institute for Fluid Dynamics, B-1640 Rhode-Saint-Genese, Belgium

and

Roland Meynart

Faculté des Sciences Appliquées, Université Libre de Bruxelles, B-1050 Bruxelles, Belgium

and

Jean Pierre Boon

Faculté des Sciences, Université Libre de Bruxelles, B-1050 Bruxelles, Belgium

and

Domenico Olivari

Von Karman Institute for Fluid Dynamics, B-1640 Rhode-Saint-Genese, Belgium

(Received 1 April 1985)

We present measurements of the dynamic behavior of macroscopic structures observed in a periodically excited air jet. The transitional, weakly turbulent state is shown to be characterized by a strange attractor with low dimensionality ($\nu = 2.6$), whereas motion of the turbulent flow is not restricted to a low-dimensional attractor.

PACS numbers: 47.25.-c, 03.40.Gc, 05.70.Ln

Low-dimensional chaos in hydrodynamic systems has been evidenced experimentally for Rayleigh-Bénard convection^{1,2} and Couette-Taylor flow.³ Chaotic dynamics was identified by the fractal dimension of the attractors, which therefore appear to be of strange type.

Such most-studied systems have confined flows with steady structures.⁴ However, the onset of chaos in Rayleigh-Bénard convection depends on the geometry of the system; e.g., in convection cells with small aspect ratios, routes to chaos may involve two or three independent modes,⁴ whereas in larger cells, quasi-periodic regimes with up to five incommensurate frequencies have been observed before chaos would set in.⁵ In this respect, free flows seem to exhibit more general behavior: In the transition to turbulence, macroscopic structures always break up into a great number of eddies with large variations in orientation, size, shape, and mean vorticity. Therefore, such flows

are also expected to be governed by a large effective number of degrees of freedom.

We have studied the onset of chaos in a free flow, i.e., an isothermal air jet at low Reynolds number, modulated by a longitudinal (along the flow axis) sinusoidal excitation.⁶ The excitation induces a periodic perturbation, with amplitude $2\pi f_0 A$, on the axial velocity. The control parameters are the amplitude, A , and the frequency, f_0 , of the excitation, and the Reynolds number, N_{Re} . The diameter of the nozzle ($D = 3$ mm) was kept constant throughout the experiments.

The unexcited jet was tested and found to be stable over an axial distance $\sim 150D$ with a well-defined Poiseuille profile at the exit (tube length $l = 80D$). Flow visualization of the excited jet (seeded with oil smoke) was performed with a stroboscoped laser-light sheet shone through the flow axis. Figure 1 shows a typical picture of the structures developed in the excit-

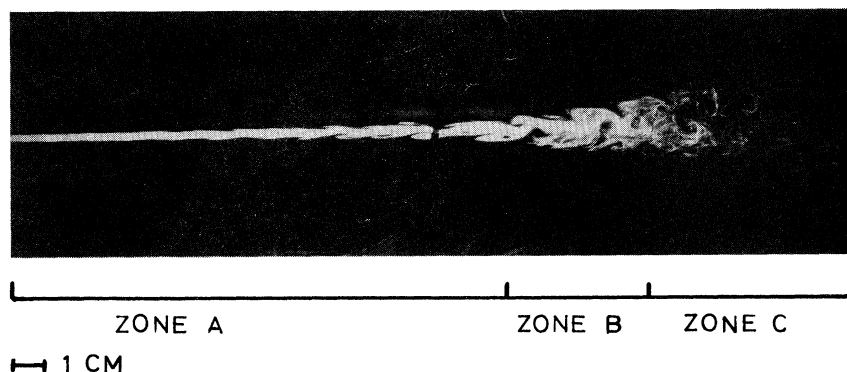


FIG. 1. Global structure of the excited jet (axially stroboscoped laser light sheet picture); $N_{Re} = 500$; $f_0 = 30$ Hz; rms velocity ratio = 2%. Zone A, laminar regime; zone B, transitional regime; zone C, turbulent regime.

ed jet, with the following sequence: steady laminar and periodic laminar zone (A), transitional (weakly turbulent) zone (B), turbulent zone (C). So the excitation induces well-defined and reproducible spatial structures in the jet⁷; the vortical structures are stable in zone A and break up into an inhomogeneous pattern in zone C via a transitional oscillating regime (zone B). This sequence was observed to be insensitive to amplitude and frequency within the investigated range ($20 \text{ Hz} \leq f_0 \leq 80 \text{ Hz}$).⁸ The present work focuses on the onset of chaos as induced by the loss of stability of the initially stable structures.

Local velocity measurements were performed with a linearized hot-wire anemometer (frequency response up to 10 kHz)⁹; each measurement produced a time series of 20 480 data points sampled at 3125 Hz. The results presented below for the transitional and turbulent regimes were obtained by adjusting the excitation amplitude A , with all other experimental parameters fixed ($D = 3 \text{ mm}$, probe position $L = 50D$, $N_{\text{Re}} = 500$, $f_0 = 40 \text{ Hz}$). For the two regimes considered here, the values of the rms velocity relative to the mean exit velocity are 2.8% and 3.3%, respectively.

Typical velocity time series and power spectra are presented in Figs. 2 and 3. In the transitional regime [Fig. 2(a)], irregularities in the time series are indications of bursts of instability in the structures; correspondingly, the power spectrum [Fig. 2(b)] shows con-

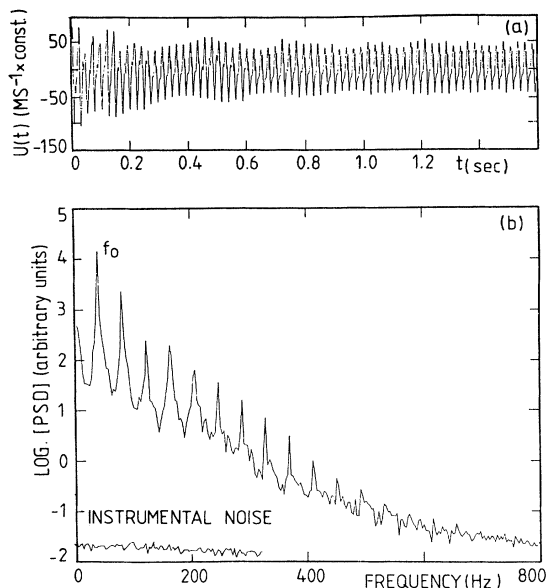


FIG. 2. Transitional regime. $N_{\text{Re}} = 500$; $f_0 = 40 \text{ Hz}$; rms velocity ratio = 2.8%. (a) Axial velocity time series (20 480 data; one-fourth of record shown; vertical scale: const = const amplification factor). (b) Power spectrum (average over twenty fast Fourier transforms computed with 1024 points; acquisition frequency, 3125 Hz).

siderable broadband noise in addition to the sharp component f_0 and its harmonics. In the turbulent regime, the velocity variations become quite irregular [Fig. 3(a)], and the peak at f_0 is the only one to remain distinguishable in the power spectrum [Fig. 3(b)].

We used the Grassberger-Procaccia algorithm¹⁰ to characterize the transitional and turbulent regimes. From the velocity time series $u(t)$, we computed the correlation integral $C(R) = \lim_{N \rightarrow \infty} N^{-2} \times$ (number of pairs of phase-space points whose distance $|\mathbf{x}_i - \mathbf{x}_j|$ is contained in a hypersphere of radius R imbedded in a d -dimensional phase space), where the state vectors \mathbf{x}_i are obtained as follows: Data points shifted with $\Delta t = p\tau$ ($1/\tau$ is the data acquisition frequency; p is the shifting parameter) in the time series were used to construct the d -dimensional state vector $\mathbf{x}(t) = \{u(t), u(t + \Delta t), \dots, u(t + (d-1)\Delta t)\}$; the imbedding dimension was varied from $d = 2$ to 16. 500 points uniformly distributed along the trajectory were correlated with all the points on the trajectory to yield $500 \times 20\,480$ correlations.

A typical plot ($p = 2$) of the dimensionality analysis for the transitional regime is shown in Fig. 4; saturation of the slope ν of $\log(C(r))$ vs $\log(R)$ is obtained for imbedding dimension $d \geq 10$ yielding dimensionality $\nu_s = 2.7$ [Fig. 4(a)].¹¹ Note that the saturation effect is well evidenced by the plot of the local slope versus $\log(R)$ for different values of d [Fig. 4(b)]. A systematic analysis was performed by variation of the time-shifting parameter p for the evaluation of the

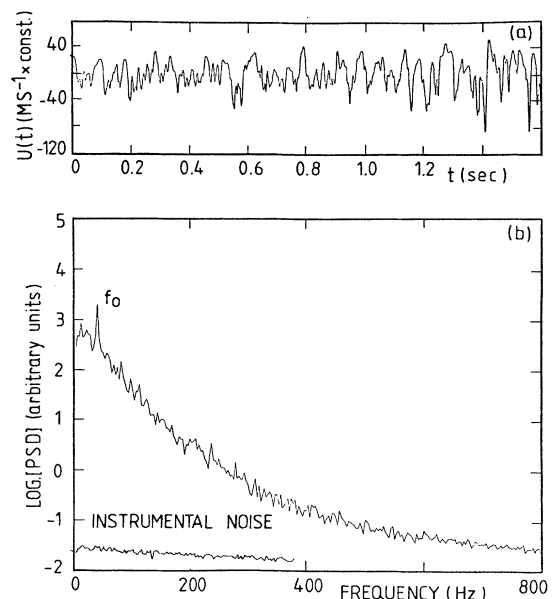


FIG. 3. Turbulent regime; same as Fig. 2 except rms velocity ratio = 3.3%.

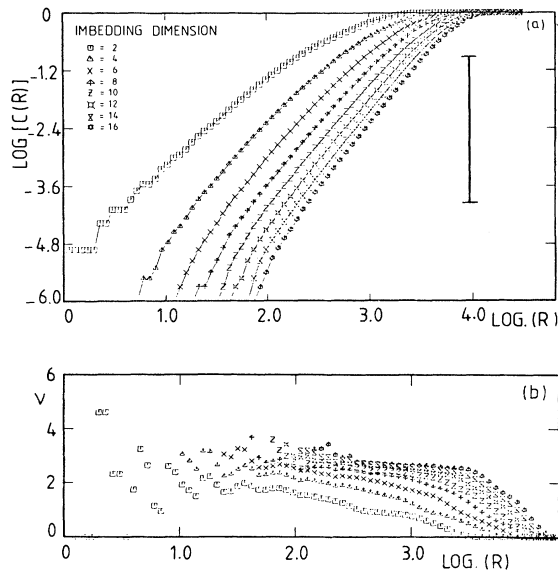


FIG. 4. (a) Dimensionality analysis for the transitional regime ($N_{Re}=500$; $f_0=40$ Hz; rms velocity ratio = 2.8%), $p=2$, $d=2$ to 16; vertical bar indicates domain of dimensionality evaluation. (b) Dimensionality vs $\log(R)$. Notice that for small R , the limited number of points yields poor average in the computation of $C(R)$, which results in a wide spread of the values of ν .

sensitivity of the dimensionality to different values of p . The results are given in Fig. 5(a). For the transitional regime, the dimensionality has average value 2.6 with a variance of 0.14. The analysis of the turbulent-regime data yields acceptable saturation of the slope ν , in the range defined by the bar as shown in Fig. 5(b) for $p=2$ ($\nu_s=3.5$).¹² However, the dimensionality is found to be p dependent as ν_s increases from ~ 2.5 for $p=1$ to ~ 7 for $p=20$, with imbedding dimension $d=16$ [Fig. 5(a)]. This observation could be interpreted as an indication of complex dynamics over a large range of time scales.¹³ Furthermore, it follows that the saturation of the slope with increasing dimension cannot be taken in general as a sufficient condition to assert the dimensionality (or even the existence) of a strange attractor. This point has also been raised by Atten *et al.*¹⁴ in a recent analysis of their study of electrohydrodynamic convection.¹

As the analysis establishes unambiguously a fractal dimension for the transitional regime ($\nu_s=2.6$), the local structure of the attractor was investigated by constructing the three-dimensional phase portrait $u(t)$, $u(t+3\tau)$, $u(t+7\tau)$.¹¹ Figure 6 shows a projection of the phase portrait and three Poincaré sections, wherefrom some degree of stretching can be noticed; however, we did not detect, in any Poincaré section, evidence of a clearly folded structure.¹⁵

In summary, we have presented a study of the

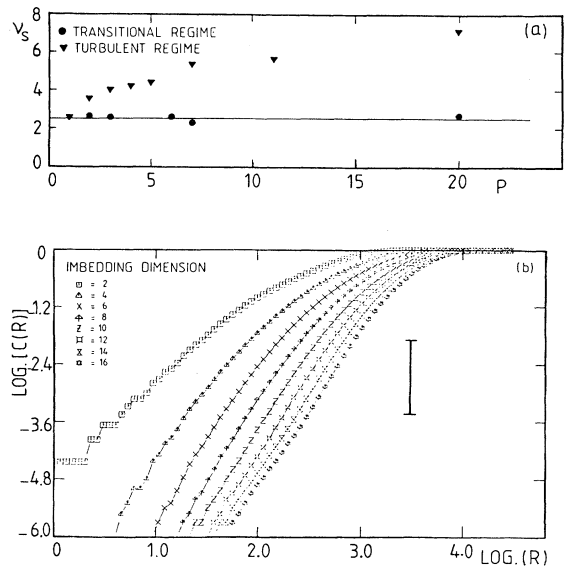


FIG. 5. (a) p dependence of slope ν_s for transitional (dots) and turbulent (triangles) regimes. (b) Dimensional analysis for the turbulent regime ($N_{Re}=500$; $f_0=40$ Hz; rms velocity ratio = 3.3%), $p=2$, $d=2$ to 16; vertical bar, same as Fig. 4(a).

dynamical behavior of the macroscopic structures observed in a nonconfined excited system undergoing transition from laminar to turbulent. Dimensionality analysis established that the transitional regime exhibits chaotic dynamics characterized by a strange attractor with low dimensionality ($\nu_s=2.6$). In the turbulent regime, the dynamics could not be identified unambiguously, as motion is probably not restricted to

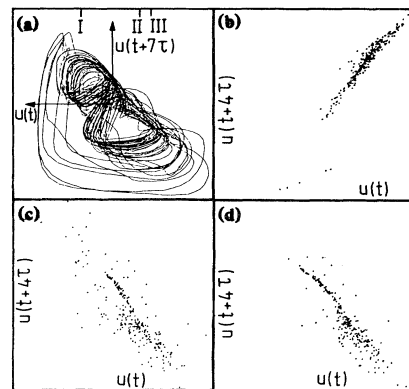


FIG. 6. Transitional regime. (a) Two-dimensional projection of phase portrait ($u(t)$, $u(t+3\tau)$, $u(t+7\tau)$) on plane ($u(t)$, $u(t+7\tau)$) (3000 points plotted out 20 480 data points). (b)–(d) Poincaré sections constructed by intersecting three-dimensional “positively” directed orbits with planes ($u(t+3\tau)$, $u(t+7\tau)$) located at I, II, III in (a), and labeled ($u(t)$, $u(t+4\tau)$) in (b)–(d).

a low-dimensional attractor. This point is presently under investigation.

We acknowledge clarifying discussions with P. Bergé, P. Couillet, M. Dubois, and G. Nicolis. Two of us (J. P. B and R. M.) are supported by the Fonds National de la Recherche Scientifique (FNRS, Belgium). This research was carried out at and supported by the Von Karman Institute in cooperation with the Université Libre de Bruxelles.

¹B. Malraison, P. Atten, P. Bergé, and M. Dubois, *J. Phys. (Paris)* **L44**, L-897 (1983).

²M. Giglio, S. Musazzi, and U. Perini, *Phys. Rev. Lett.* **53**, 2402 (1984).

³H. L. Swinney, in *Fundamental Problems in Statistical Mechanics VI*, edited by E. G. D. Cohen (North-Holland, Amsterdam, 1984); A. Brandstätter *et al.*, *Phys. Rev. Lett.* **51**, 1442 (1983).

⁴M. Dubois and P. Bergé, *J. Phys. (Paris)* **42**, 167 (1981).

⁵R. W. Walden, P. Kolodner, A. Passner, and C. M. Surko, *Phys. Rev. Lett.* **53**, 242 (1984).

⁶Experimental details will be reported elsewhere.

⁷The structures are periodic in time while spatially developing downstream. Figure 1 shows a picture of stroboscopically "frozen" structures.

⁸An increase in f_0 and/or A shortens the axial distance at which the transition to turbulence takes place, but does not modify the sequence of the successive regimes; the same

observation holds for an increase in N_{Re} with fixed f_0 and A .

⁹As test measurements showed excellent agreement with LDV data [G. W. Rankin, K. Sridhar, M. Arulraja, and K. R. Kumar, *J. Fluid Mech.* **133**, 217 (1983)], we are confident that the flow was not perturbed by the probe.

¹⁰P. Grassberger and I. Procaccia, *Phys. Rev. Lett.* **50**, 346 (1983), and *Physica* **9D**, 189 (1983).

¹¹We checked the periodic laminar regime ($N_{Re} = 1000$; $L = 16D$; $f_0 = 40$; rms velocity ratio = 2.5%); time series produced trajectories well confined on a limit cycle and $C(R)$ yielded a well-defined dimensionality $\nu_x = 1.1$ (the excess value 0.1 could be due to weak incipient nonlinearities in the flow regime).

¹²This method of evaluation was preferred to a plot of the form of Fig. 4(b) which in this case yielded no unambiguous saturation value because of larger variations in the local slope (computed by central differences).

¹³However, operationally, this p dependence may result from too low an upper bound of the imbedding dimension in performance of the dimensionality analysis ($d \geq 2\nu + 1$); F. Takens, in *Dynamical Systems and Turbulence, Warwick 1980*, edited by D. A. Rand and L.-S. Young, *Lecture Notes in Mathematics*, Vol. 898 (Springer-Verlag, Berlin, 1981), p. 366. We also suspect a possible connection between this effect and the data acquisition frequency.

¹⁴P. Atten, J. G. Caputo, B. Malraison, and Y. Cagne, "Determination of Attractor Dimension for Various Flows," to be published.

¹⁵A larger number of intersection points should be necessary to ascertain the presence of folding. Attempts to construct significant return maps failed to produce typical curves with a maximum.

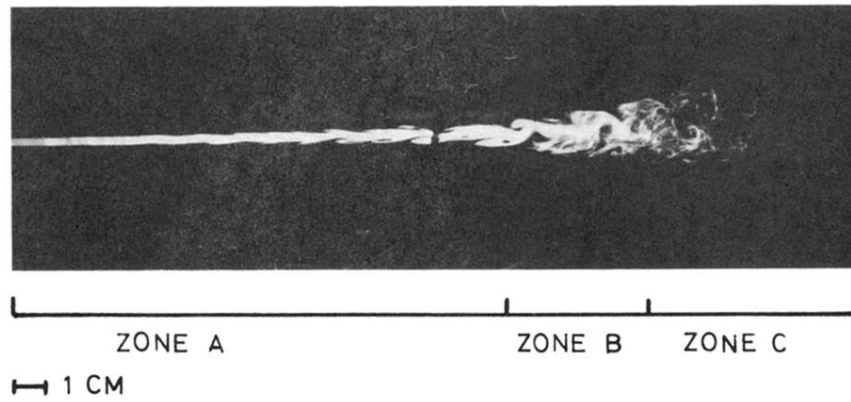


FIG. 1. Global structure of the excited jet (axially stroboscoped laser light sheet picture); $N_{Re} = 500$; $f_0 = 30$ Hz; rms velocity ratio = 2%. Zone A, laminar regime; zone B, transitional regime; zone C, turbulent regime.